Journal of Power Sources 196 (2011) 7002–7005

Contents lists available at ScienceDirect

Journal of Power Sources

journal homepage: www.elsevier.com/locate/jpowsour

Short communication

Large-format lithium-ion batteries for electric power storage

H. Haruna[a], S. Itoh[a], T. Horiba[a,*], E. Seki[b], K. Kohno[b]

[a] Shin-Kobe Electric Machinery Co., Ltd., 2200 Oka, Fukaya, Saitama 369-0297, Japan
[b] Hitachi Research Laboratory, Hitachi, Ltd., 7-1-1 Ohmikacho, Hitachi, Ibaraki 319-1292, Japan

ARTICLE INFO

Article history:
Received 14 August 2010
Received in revised form 14 October 2010
Accepted 18 October 2010
Available online 26 October 2010

Keywords:
Electric power storage
Lithium ion battery
Manganese spinel
Hard carbon
Life performance

ABSTRACT

We have been developing lithium-ion batteries for electric power storage and have chosen cell chemistries having a high energy density and long life. The cell chemistry consisted of a positive electrode containing a lithium–manganese spinel or a mixture of it with a layered-manganese-based material, and a negative electrode containing a hard carbon. The 8 Ah-class cells consisting of these cell chemistries showed that their extrapolated lives were long enough to withstand a cycling load for 10 years of use. A comparison of the cycle life data with the storage life data suggested the possibility to separate the capacity fading caused only by the storage and that only by the cycling, which is expected to be the basis of a prediction method for the calendar life. However, much work still needs to be done to achieve it. We also manufactured two types of 100 Ah-class cells as an experiment based on the results for the 8 Ah-class cells. They showed specific energies of 100 Wh kg^{-1} and 106 Wh kg^{-1}.

1. Introduction

It is important to exploit natural energies in order to cope with the dilemma between economic growth and global warming. One of the most serious issues is how to minimize the loss in energy from production to consumption. In other words, how to store, recover, and buffer energy during its life. Battery technology is expected to be one of the promising solutions for this issue, because it has the features of a high energy efficiency, compactness, easy expansion in scale, etc. Among the various kinds of batteries, lithium-ion batteries are considered to have excellent characteristics to be applicable for these purposes.

Therefore, we have been participating as a battery developer in the NEDO (New Energy and Industrial Technology Development Organization) project, "Development of Electric Energy Storage System for Grid-connection with New Energy Resources". Its purpose is to further expand the introduction of photovoltaic and wind power generation systems [1]. It is a five-year project from FY2006 to 2010 [2]. We will show and discuss some of our results achieved in the NEDO project with 8 Ah-class small cells and 100 Ah-class cells.

2. Experimental

The cell chemistries we tested consisted of a positive electrode containing a partially substituted lithium-manganese-spinel ($LiMn_{2-X}M_XO_4$) or a mixture of it with a layered-manganese-based material ($LiMn_{1-X-Y}M_XN_YO_2$), and a negative electrode containing a pitch-based hard carbon or a granulated natural graphite. The positive electrode was formed on an aluminum foil by coating it with an active material mixture slurry containing the active material, a conductive carbon material and a PVDF (polyvinylidene difluoride) binder. The negative electrode was formed on a copper foil by coating it with an active material mixture slurry containing the active material and a PVDF binder. After drying, pressing and slitting, both electrodes were wound with separators into a cylindrical electrode assembly. The separator was an ordinary polyolefin microporous sheet. The wound electrode assembly was placed in a cell can made of Ni-plated steel and crimped with a gasket and a cap after the injection of an electrolytic solution. The electrolytic solution consisted of a mixture of organic carbonate solvents and a lithium hexafluorophosphate salt ($LiPF_6$) at a 1 mol L^{-1} concentration. The specifications of the three kinds of 8 Ah-class small cells, Cells A, B, and C, are summarized in Table 1. The cell dimensions are 40 mm in diameter and 108 mm long [3].

Cylindrical 100 Ah-class cells were designed using the cell chemistry of Cell A and Cell B, and the other materials, such as the separator and electrolytic solution, were the same as those for the 8 Ah-class cells. The wound electrode assembly was placed in a cell can made of a stainless steel cylinder and sealed by laser welding with the caps on the both end of the cylinder followed by the injection of the electrolytic solution and the hermetic seal of the injection hole. The cell dimensions were 67 mm in diameter and 381 mm long [4].

The 8 Ah-class cells were cycled at 25 °C in an isothermal box using the Regenerative Charge /Discharge Cycler, 5V300A,

* Corresponding author. Tel.: +81 48 546 1107; fax: +81 48 546 1138.
E-mail address: t.horiba@shinkobe-denki.co.jp (T. Horiba).

0378-7753/$ – see front matter © 2010 Elsevier B.V. All rights reserved.
doi:10.1016/j.jpowsour.2010.10.045

Table 1
Specifications of 8 Ah-class cells.

	Electrode materials		Symbol	Energy density (Wh kg^{-1})
	Positive	Negative		
Cell A	Li–Mn–spinel	Hard C	Sp/HC	80
Cell B	Li–Mn–spinel/layered[a]	Hard C	Mixed/HC	100
Cell C	Li–Mn–spinel/layered[a]	Natural graphite		130

[a] Layered: layered-manganese-based material.

Takasago, Ltd. The cells were charged at 4 A to 4.2 V in the CC–CV (constant current–constant voltage) mode for 3 h. The discharge current was 4 A and the cut-off voltage was 2.7 V. The rest time between the charge and discharge, or discharge and charge, was 20 min.

These cells were also stored at 25 °C or 50 °C in an isothermal box after being charged to 3.9 V or 4.2 V. All cells were charged and discharged to estimate the capacity fading after storage for 30 or 60 days.

The 100 Ah-class cells were tested at 25 °C in an isothermal box using the Charge /Discharge Cycler, IEM Co., Ltd., at 45 A to 4.2 V in the CC–CV mode for 3 h. The discharge current was 45 A and the cut-off voltage was 2.7 V. The rest time between the charge and discharge, or discharge and charge, was 20 min.

3. Results and discussion

We began by choosing the cell chemistry to meet the target for the NEDO project, such as a specific energy of 50–200 Wh kg^{-1}, 5 kW module with 100 Ah-class single cells and a 10-year life. The discharge characteristics of the cells are shown in Fig. 1. The shape of the voltage curve for Cell C is quite different from those of the other two because of the negative electrode material. The rated capacities of the three cells were 6.7, 7.8 and 10.2 Ah, and their specific energies are shown in Table 1. Although Cell C showed a high capacity and specific energy, we excluded this cell chemistry in the following study because of its poor cycle life test results. Nevertheless, natural graphite is a very promising material for large-format applications based on its low cost. Further study is still needed for us to realize a long-life Li-ion battery using a graphite-based anode.

Fig. 2 shows the storage performance of Cell A. Capacity fading was explicitly dependent on the temperature and cell voltage, that is, the state of charge. In other words, the higher the storage temperatures or cell voltage, the greater the capacity fading, and the temperatures are more effective than the voltage. Fig. 3 shows the storage performance of Cell B, which has the same tendency as shown in Fig. 2. However, the percent of capacity fading for Cell B is much lower than that for Cell A. Also, the effect of the cell voltage during storage was reduced to a very low level.

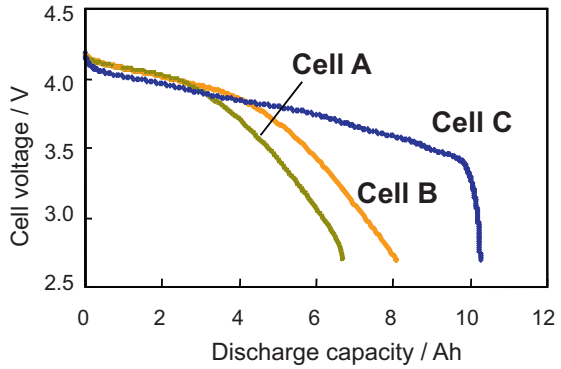

Fig. 1. Discharge characteristics of 8 Ah-class single cells.

This difference seems to be caused by the addition of a layered-manganese-based material to the lithium–manganese–spinel, and the addition presumably reduced the manganese dissolution from the lithium–manganese–spinel in the cathode at high temperatures and at a high state of charge [5,6].

Fig. 4 shows the cycle performances of Cell A and Cell B at 25 °C. Both Cell A and Cell B showed a similar capacity fading. After 1500 cycles, Cell A retained 78% of the initial capacity, while Cell B retained 84%. Fig. 5 is the modified cycle performance derived from Fig. 4; the vertical axis is converted into relative capacity versus the initial, and the horizontal axis is also converted into the square root of the cycle time by hours with the ratio of 6 h per cycle. The capacity fading showed a linear function of the square root of the cycle time [7]. The correlation coefficients, R^2, were 0.994 for Cell A and 0.992 for Cell B. A similar linear relationship was already reported as an oxide film growth on the surface of metal, called the tarnish-

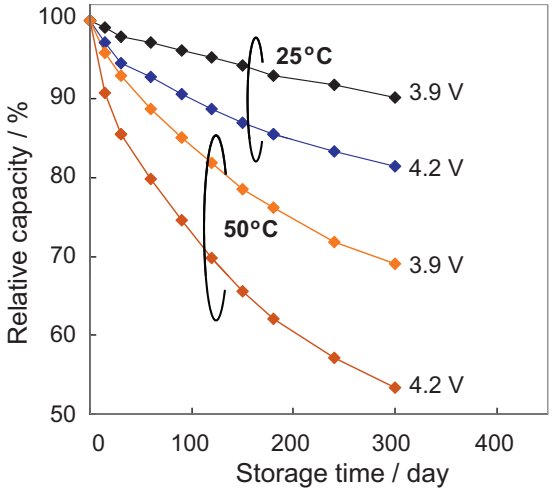

Fig. 2. Storage performance of 8 Ah-class Cell A.

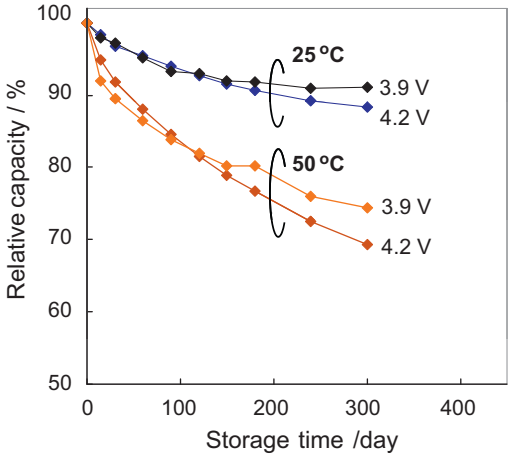

Fig. 3. Storage performance of 8 Ah-class Cell B.

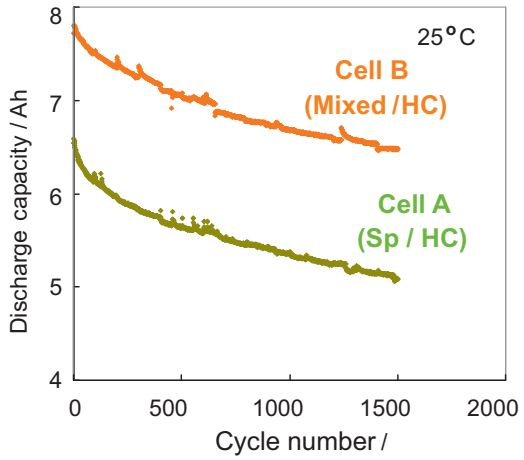

Fig. 4. Cycle performances of 8 Ah-class cells.

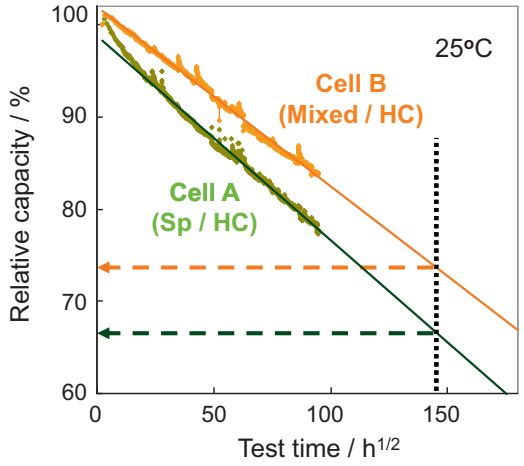

Fig. 5. Modified cycle performances of 8 Ah-class cells.

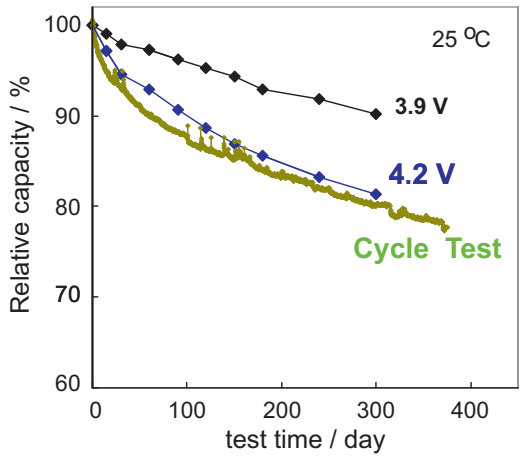

Fig. 6. Comparison of cycle and storage test data for Cell A.

ing reaction [8], which proceeds in proportion to the square root of time, and the rate determining step of the reaction is the diffusion of oxygen molecules in the film. Therefore, we developed the hypothesis that the capacity fading mechanism is a kind of film formation on the surface of the active material particles based on the analogy of the case reported in Ref. [8].

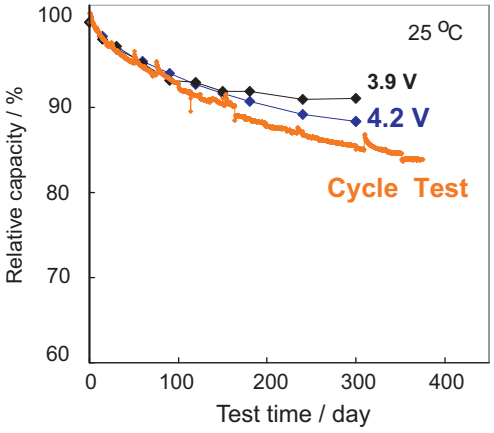

Fig. 7. Comparison of cycle and storage test data for Cell B.

The target for the cell life in this project is 10 years with a capacity over 60% of the initial. The 10-year use with one cycle per day corresponds to 3650 cycles, which thus requires 21,900 h and is equal to 148 square root hours. According to the previous discussion, we assumed that the linear relationship should be valid even after longer cycles, i.e., after 1500 cycles or 9000 h. Thus, the extrapolated results shown in Fig. 5 indicate that both Cell A and Cell B will exceed the target; Cell A will retain 66% of the initial capacity and Cell B will retain 73%. These results mean that both the Cell A and Cell B chemistries are capable of withstanding a cycling load for 10 years of use. However, the actual use for 10 years definitely depends on the rest time along with the cycling operation time, therefore, the fading of the rest time should also be included in the exact prediction of the battery life time. We transformed the storage test data of Cell B shown in Fig. 3 into the same form as shown in Fig. 5 and obtained a similar linear relationship. Using this result, we initially tried to estimate the 10-year use life, although the additivity of the capacity fading of the cycle test and storage test has not yet been proved. The total rest time over ten years corresponds to 65,700 h and is equal to 256 square root hours based on the assumption of a 6-h operation per day. During this time, the capacity fading for the cell stored at 3.9 V will be 15%. 3.9 V is the midpoint of the cycle test voltage range, therefore, it seems reasonable to regard 3.9 V as the average voltage during storage. If the additivity of the cycle test fading and storage test fading is valid, the capacity of Cell B after a 10-year actual use will be 58% of the initial. Although 58% is less than the target of 60%, the difference is only 2%. Another calculation indicates that the time to reach 60% of the initial capacity will

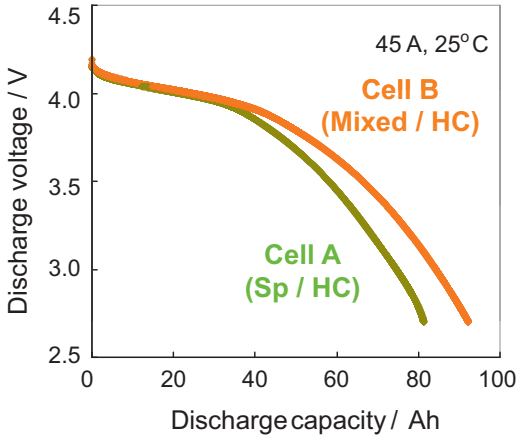

Fig. 8. Discharge characteristics of 100 Ah-class single cells.

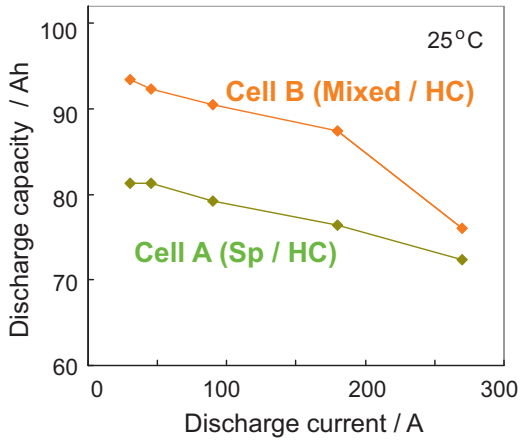

Fig. 9. Discharge current characteristics of 100 Ah-class single cells.

be 9.2 years. Based on these results, as the preliminary results, it is rather encouraging that the target can be attained in the future.

Both Figs. 6 and 7 compare the capacity fading between the storage tests and cycle test using the same scale of spent time for the tests. The capacity fading of Cell A shown in Fig. 6 is greater than that of Cell B shown in Fig. 7. The fading tendencies in the two figures are almost the same; the capacity fading during cycling is greater than those during storage at 3.9 V and 4.2 V, or the cycling is more stressful than the storage. The cell voltages during the cycle test changed from 4.2 V to 2.7 V. This voltage range defined 100% state of charge (SOC) to 0% SOC. Accordingly, 3.9 V is the cell voltage at 50% SOC and is also the average voltage during cycling. If the capacity fading during the cycle test is caused by the stress of the charge–discharge cycling and by the storage time, and if the additivity between these effects is valid, the differences between the 3.9 V-storage and cycle test in Figs. 6 and 7 correspond to the capacity fading caused only by the stress of the charge–discharge cycles. This is just a rough estimation, therefore, a further study is necessary to verify the additivity of the cycling and storage test data for the life prediction and to enable us to estimate an accurate calendar life.

We developed the 100 Ah-class single cells based on the results described above. Fig. 8 shows the discharge characteristics for the single cells of the Cell A and Cell B chemistries. The discharge capacity at 45 A for Cell A was 81 Ah, and that for Cell B was 93 Ah, which corresponded to the specific energies of 100 and 106 Wh kg^{-1}. Fig. 9 shows the current dependence of the discharge capacity. The discharge capacities at 270 A, around a 3C rate, were 89% for Cell A and 91% for Cell B versus those at 45 A. We are further testing these cells including life tests, and also to assemble 5 kW-class modules of 12 cells to evaluate their practical performance. The results will be reported in our next paper.

Acknowledgements

This work was supported by NEDO (New Energy and Industrial Technology Development Organization). The authors gratefully acknowledge those who participated in the projects.

References

[1] H. Haruna, S. Itoh, T. Hirasawa, E. Seki, K. Kohno, Proc. 49th Battery Conf. 1F09, Osaka, November 4–6, 2008.
[2] S. Yumitori, Proc. Abstracts 15th International Meeting on Lithium Batteries Abstract #3, Montreal, June 28–July 2, 2010.
[3] T. Horiba, K. Hironaka, T. Matsumura, T. Kai, M. Koseki, Y. Muranaka, J. Power Sources 119–121 (2003) 893–896.
[4] T. Horiba, K. Hironaka, T. Matsumura, T. Kai, M. Koseki, Y. Muranaka, J. Power Sources 97–98 (2001) 719–721.
[5] Y. Xia, M. Yoshio, J. Power Sources 66 (1997) 129–133.
[6] S. Komaba, N. Kumagai, Y. Kataoka, Electrochim. Acta 47 (2002) 1229–1239.
[7] H. Yoshida, N. Imamura, T. Inoue, K. Komada, Electrochemistry 71 (2003) 1018–1024.
[8] K. Fischbock, Metallwirtsch 14 (1935) 733–753.